Materials Research Proceedings 28 (2023) 231-238 https://doi.org/10.21741/9781644902479-25

Modelling the forming of tailored fibre placement preforms: A tetrahedral part with final orthotropic orientations

SIMON Jessy[1,2,a *], HAMILA Nahiene[1,b], BINÉTRUY Christophe[2,c] and COMAS-CARDONA Sébastien[2,d]

[1]IRDL, UMR CNRS 6027, ENI Brest, F-29200, Brest, France

[2]Nantes Université, Ecole Centrale Nantes, CNRS, GeM, UMR 6183, Nantes, F-44000, France

[a]jessy.simon@enib.fr, [b]nahiene.hamila@enib.fr, [c]Christophe.Binetruy@ec-nantes.fr, [d]sebastien.comas@ec-nantes.fr

Keywords: Tailored Fibre Placement, Forming, Finite Element, Orthotropic Design

Abstract. Forming of conventional reinforcements to manufacture 3D fibre-reinforced composite parts with complex geometries is limited by the architecture of the reinforcement made of initially straight fibres. On the opposite preforms obtained by Tailored Fibre Placement (TFP) are made of curvilinear fibre tows maintained on a backing material through stitching. In theory, the degree of freedom offered by TFP allows to form doubly-curved parts from preforms whose designs are determined from the desired final fibre orientations. In practice, it requires numerical tools to determine the design of the flat TFP preforms from the desired 3D parts, known as flattening. However, flattening is a virtual process which cannot be validated directly. Besides, the behavior of TFP preforms during forming has never been studied. Consequently, developing a numerical model to predict the formability of TFP preforms was considered as of first importance. Moreover, numerical forming can be required in a flattening algorithm [1]. Based on the Finite Element Method, a TFP preform is modelled at the fibre tows scale using 2-node beam elements. The stitching yarn, which ensures the cohesion of the layers, is modelled implicitly using an embedded element approach. The backing material is removed. A full-scale simulation of forming is experimentally validated. A tetrahedral shape, which corresponds to a corner bracket, is used to demonstrate the potential of TFP preform forming. An orthotropic design of the final part is achieved without defects using a simple forming device, which represents important progress in the field [2].

Introduction

Forming of conventional reinforcements to manufacture 3D fibre-reinforced composite parts with complex geometries is inherently limited by the architecture of the reinforcement made of initially straight fibres. As opposed to regular fabrics, fibrous reinforcements made by Tailored Fibre Placement (TFP) are made of curvilinear fibre tows maintained on a backing material through stitching. In theory, the degree of freedom offered by TFP allows to form doubly-curved parts from preforms whose designs are determined from the desired final fibre orientations. The flattening step which consists in determining the flat pattern from the desired final part is virtual and can only be computed numerically for complex parts. However, developing such a numerical tool would require prior knowledge of the behavior of a TFP preform during forming (or unforming). Therefore, it is of primary importance to investigate the forming behavior of TFP preforms before focusing on the flattening step. Moreover, Sun et al. [1] shows the option to use a forming numerical tool as a step of the flattening operation to determine the reverse trajectory to be imposed to the final configuration in case of double diaphragm forming. This is why this work focused on developing a numerical tool to model the behavior of TFP preforms during forming.

Previous work on TFP investigated the advantages of aligning fibres with the principal stress directions in 2D parts [3-5]. For instance, the stress concentration in notched plate can be removed by using curvilinear path circumventing geometric discontinuities [6-9]. The work by Uhlig et al. [10] compared the strength of TFP and Non-Crimp Fabrics (NCF) open-hole laminates using cyclic and tensile tests and showed similar performances. Examples of work focusing on the manufacturing of 3D shapes using TFP is quite limited. Takezawa et al. [11] manufactured a car hood from two distinct layers with optimal orientations based on Gaussian curvatures considerations. Rihaczek et al. [12] determined optimized flat pattern to form a stool by bending. This work follows a double objective. The first one is to demonstrate the ability of manufacturing 3D orthotropic parts from specifically designed flat TFP preforms which cannot be achieved by forming conventional textiles and will therefore represent a major improvement in the field of fibrous reinforcement forming. The second one is to propose a first efficient model to simulate the forming of TFP preforms. Validation of the proposed modelling strategy is addressed by experimental and numerical forming on a tetrahedral shape. This shape has a highly double curvature and corresponds to a corner bracket widely used to design composite structures. The forming of conventional reinforcements on this shape has been largely studied [13,14] and showed the complexity of manufacturing such a shape without defect.

This paper is organized as follow. The second section describes the experimental work on TFP preform forming on a tetrahedral shape with quantitative measurements. The next section introduces the finite element modelling strategy. Finally, the last section presents the results of the forming simulation and its comparison with the experimental forming.

Experimental Forming on a Tetrahedral Shape

TFP preform architecture.

A TFP preform is built from a continuous fibre tow deposited on a flat backing material along curvilinear trajectories and maintained in place through a zig-zag stitching pattern as illustrated in Fig. 1. The thickness of the preform is achieved through stacking of several layers. When manufacturing a TFP preform, the stitch length, width and tension can be varied. Depending on the layout pattern, intra-layer and inter-layer overstitching create additional bonding between the fibre tows in a layer and between layers. The numerous interactions between the different components of a TFP preform, namely, the backing material, the fibre tows and the stitching yarn, inherently make its realistic modelling difficult. Moreover, depending on the nature of the backing material, the formability of the TFP preform can be limited. When using a thermoforming process, a non-woven polymer film which will add polymer in the final part is a good choice. However, in this work the forming experiment are carried-out at ambient temperature. Since the cohesion conferred by the stitching yarn between the layers was deemed sufficient, the backing material was removed prior to forming.

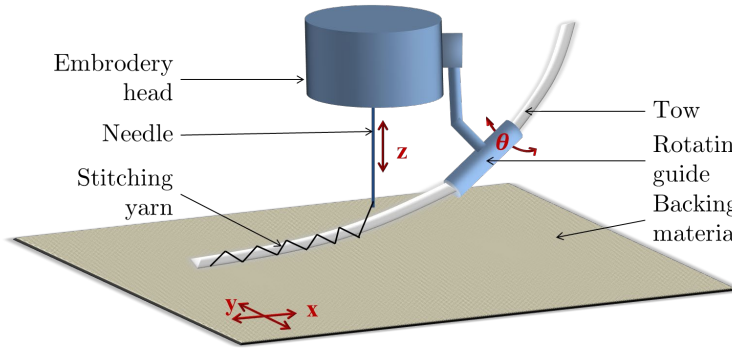

Fig. 1. TFP principle [2].

Material and manufacturing of the TFP preforms.

The TFP preforms where manufactured at IRT Jules Verne using the TFP ZSK © CMCW 0200-900D-2500 embroidery machine. A PolyVinyl Alcohol (PVA) water soluble film was used as backing material and removed by washing. Then, the TFP preform were dried in an oven at a temperature of 60◦C. The 2690 tex PET/E-glass continuous tow (from P-D-Glasseiden GMBH,

Oschatz, Germany) was stitched onto the PVA film (Gunold® Solvy film 80, Stecker) using a 24 tex PET stitching yarn (Serafil fine, Amman). The stitching length and width were set to 2.5 mm and the stitching tension to 5 10^{-2} N.

TFP preform design.

The objective is to obtain an orthotropic configuration in the final tetrahedral part. In practice, the determination of the flat pattern from the desired final configuration, namely, the flattening step, would require a numerical tool for complex geometries [1]. However, for the case of a tetrahedral shape, the flat pattern was determined analytically based on the assumption of the fibre tows inextensibility. Fig. 2 (a) shows the desired configuration of a 2-layer TFP preform. On each face of the tetrahedral shape, a 0/90° orientation is achieved. Since fibre tows are aligned with the three edges which converge through the vertex of the tetrahedron, their length must be conserved in the flat configuration. These constraints are satisfied with an angle of 120° between the edges in the flat configuration Fig. 2 (b). Therefore the fibre tows have initially an angle of 120° between the two layers on each face. During the forming step, a uniform in-plane shear deformation characterized by an angle of 30° is expected. Fig. 3 shows the flat pattern with is split into two layers. It should be noticed that several combinations of 2-layer lead to this flat pattern. As it will be highlighted at the end of this section, it was noticed to late that the chosen one was not optimal.

Forming device.

The forming device shown in Fig. 4 is composed of a tetrahedral punch mounted on the cross head of a universal testing machine (AGXplus by Shimadzu). Two transparent square plates (550 mm × 550 mm × 10 mm) made of poly(methyl methacrylate) are used as blank-holder. One plate is fixed within a metallic frame and the other lies directly onto the preform and only applies its self-weight. A pin system prevents the movable plate of the blank holder from moving in the plane. The tetrahedral part of the punch is 120 mm high and on top of a 20 mm thick base. The stroke punch stroke is 140 mm with a speed of 15 mm/min.

Quantitative measurements.

Optical measurements were carried out to compare the results with the forming simulations presented the last section using a camera positioned along the displacement axis of the punch which takes a picture every 2~mm. This setup allows visualizing the 2D displacement field orthogonal to the punch displacement. Moreover, at the end of the experiment, a picture of one face of the punch was taken to measure the inter-layer angle. Red-ink markers were drawn on the TFP preform in order to compute the 2D displacement field and a python script based on the open-source image-processing library OpenCV was used to track the position of these markers. This 2D displacement field allows extracting the preform contour for comparison with the simulation results in the last section.

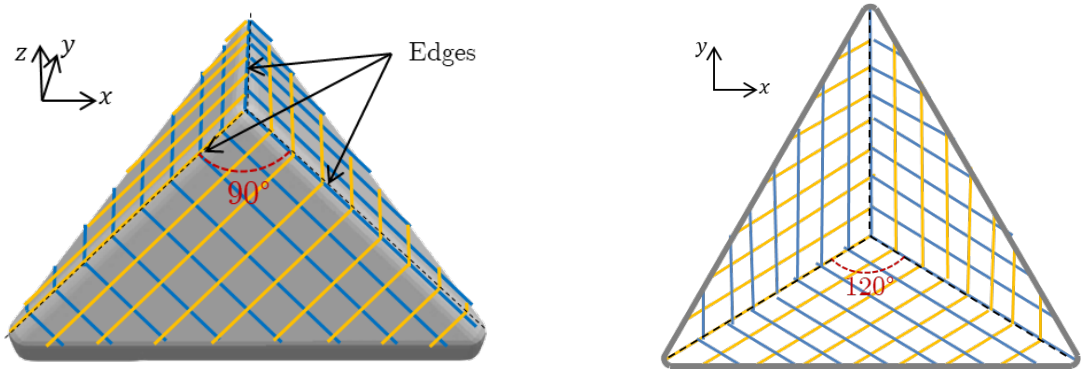

(a) (b)

Fig. 2. Desired orthotropic configuration (a) and analytically determined flat pattern (b).

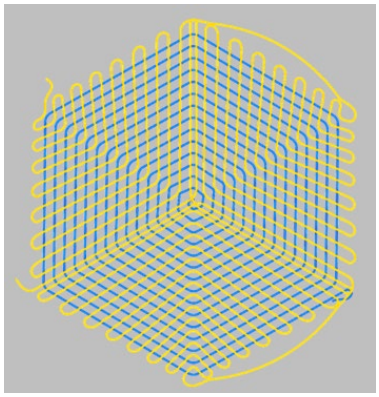

Fig. 3. TFP preform flat design (with reduced number of fibre tows for visibility).

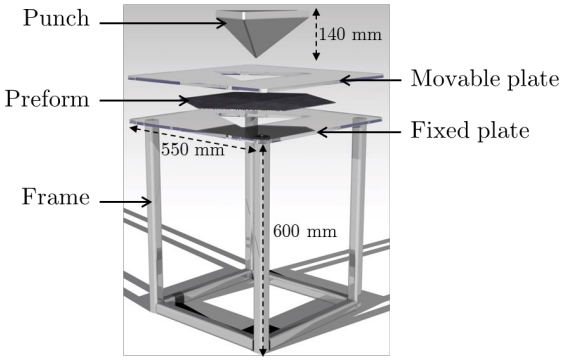

Fig. 4. Forming device.

Results.

The final configuration of the forming process as well as the force-displacement curve is shown in Fig. 5. No apparent defects such as wrinkles or fibre tow slippage were noticed. The force-displacement curve shows a first phase with a slow increase until 120 mm before increasing rapidly once contact with the thick base (120-140 mm) is established. Therefore, the minimal blank-holder used was sufficient to obtain a final configuration free of defects. Concerning the final inter-layer orientation, from the picture taken on one face, the trajectory of the fibre tows was extracted manually by drawing curves using Inkscape and saved as a svg file for post-processing. Then a python script extracted the curves representing each fibre tow and the angle at the intersection of two fibre tows was computed. Fig. 6 (a) shows the extracted trajectories and while Fig. 6 (b) presents a nice distribution of the inter-layer angle around 90°. Considering a normal distribution of the angles, a mean angle of 90.72◦ with a standard deviation of 4.31◦ is obtained. However, it must be noticed that due to the choice of the layers to obtain the flat TFP pattern, the fibre tows are parallel along the symmetry line of the faces. Another choice for the layer layout which eliminates this orientation defect was noticed too late.

(a)

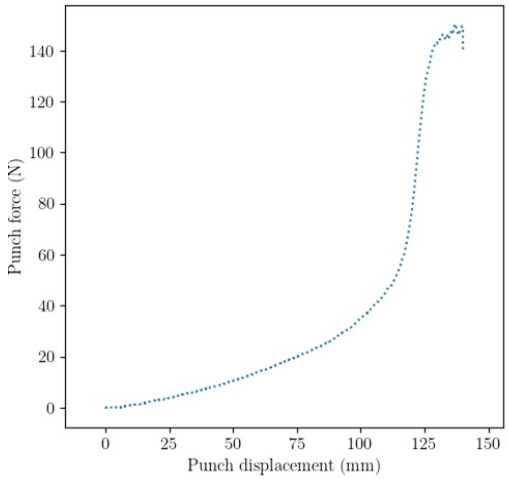

(b)

Fig. 5. Final configuration of the forming process (a), force-displacement curve (b).

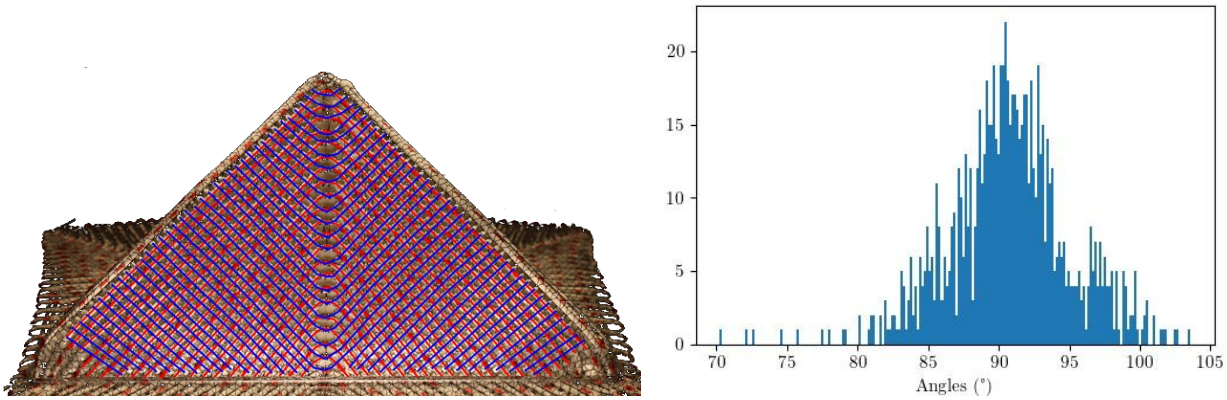

(a) (b)

Fig. 6. Manually extracted trajectories of the fibre tows on a face (a), inter-layer angle distribution on this face computed at fibre tows intersections.

Finite Element Model of a TFP Preform

Modelling strategy.

The model developed to simulate the forming of a TFP preform without backing material is based on the finite element method. Since the backing material is removed prior forming in this work or in a melted state when a thermoforming process is used, its contribution is neglected. To take into account the flexibility offered by the TFP technology in the preform design, it was chosen to use a semi-discrete approach where the preform is modelled at the scale of the fibre tows.

Hypothesis.

In this model, the fibre tows are considered to be quasi-inextensible. Although the backing material is removed prior forming, the stitching yarn is assumed to ensure the cohesion between the layers thanks to inter-layer overstitching.

Fibre tows.

The fibre tows are modelled as a continuum medium using 2-node shear-flexible beam element. The initial formulation of this type of element can be found in [15-17]. Since fibre tows cannot be considered as a perfect continuum medium, the section moduli, which relate the cross-section forces and moments to its deformation and curvatures, are considered to be independent. A high value of the tensile modulus ensures a weak enforcement of the quasi-inextensibility constraint.

Stitching yarn.

The stitching yarn is the component of a TFP preform whose contribution is the most difficult to take into account. To avoid burdensome computations implied by a realistic modelling of the stitching yarn and its interactions with the fibre tows, it is modelled implicitly as an embedded constraint between crossing fibre tows of adjacent layers. In other words, the stitching yarn is assumed to act as a perfect bond between fibre tows of adjacent layers which intersect. The embedding constraint principle is illustrated in Fig. 7 where two fibre tows intersect. To apply this constraint a node is required at the intersection between the elements of the lower fibre tow and those of the upper fibre tow. On the kinematic side, the displacement of this node is computed as function of the displacements of the lower beam element it is embedded in (host element). As a consequence, forces which are computed at this embedded node are transferred on the nodes of the host beam element. To take into account the resistance to rotation between crossing fibre tows, a linear torsional spring is added at each intersection. The vertical offset between the two crossing fibre tows in Fig. 7 is only for visibility purpose.

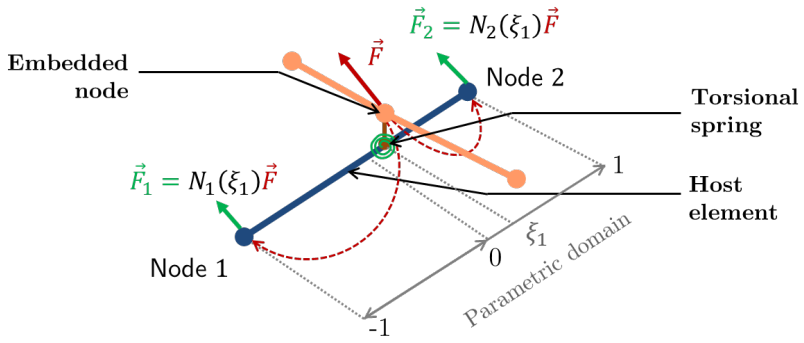

Fig. 7. Embedding constraint principle: Transfer of forces from an embedded node to the nodes of its host element.

TFP preform model.

Therefore, in this work, a 2-layer TFP preform without backing material is considered where the fibre tows are modelled explicitly using 2-node shear flexible elements and the stitching yarn is modelled implicitly through an embedding constraint where the fibre tows of adjacent layers intersect each other. The resistance to in-plane shear is taken into account through a linear torsional spring at these intersections.

Numerical Forming on a Tetrahedral Shape

Material parameters.

The model requires six independent material parameters for the beam elements corresponding to the six independent deformation modes (one for tension/compression, 2 for transverse shears, 2 for flexions and one for torsion). An additional parameter is required for the resistance to rotation between crossing fibre tows. No characterization of these material parameters was carried-out and their estimation is given in Table. 1.

Table. 1 Values of the material parameters for the beam elements and the torsional springs.

Modulus	**Tensile**	**Transverse shear 1**	**Transverse shear 2**	**Flexion 1**	**Flexion 2**	**Torsion**	**Torsional spring**
Value	1400	700	700	1	0.1	1	1
Unit	kN	kN	kN	kN mm²	kN mm²	kN mm²	N mm

Finite element solver.

A research code based on an explicit scheme is used to simulate the forming process with a time step of 10^{-4}s. The contact interactions between the TFP preform and the tools, namely, the tetrahedral punch and the blank-holders are solved using a forward increment Lagrangian multipliers method.

Finite element model.

The first layer is composed of beam elements of 2.5 mm. The second layer is meshed with the same element size but nodes additional nodes are required at intersections with the elements of the first layer. These additional nodes are embedded in the corresponding host elements of the first layer. The total number of beam elements is 22190 and the simulation runs in 12 h using four cores of an Intel(R) Core(TM) i7-8750H CPU 2.20 GHz processor. A friction coefficient of 0.2 between the fibre tows and the forming tools was chosen for simplicity even though it might be different since the blank-holders are made of different polymers. A displacement of 140 mm is imposed to the punch. Concerning the blank-holder, the fixed part is clamped and the movable part can only move along the punch axis as in the experiment. Rigid surfaces are used to model the tools.

Results.

A comparison between the experiment and the simulation is shown in Fig. 8 (a). In this figure, the contours of the preform in the experiment and in the simulation are superposed on the left part and shows good agreement. In Fig. 8 (b), the inter-layer angle field on one face of the punch is displayed. The colormap shows a distribution of the inter-layer angle around 90° as expected, except along the line of symmetry of the face as explained in the experimental section.

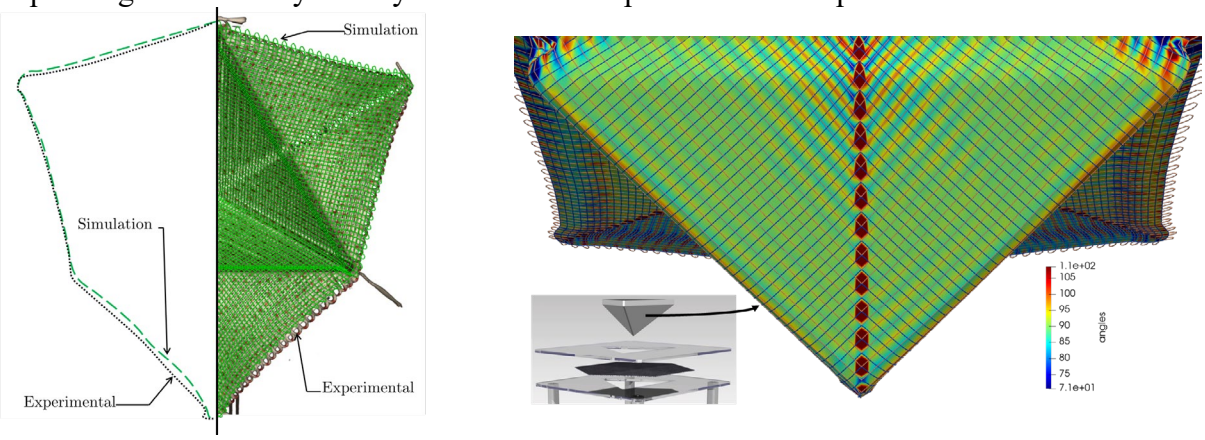

(a) (b)

Fig. 8. Superposition of the preform contour in the experiment and simulation (a), inter-layer angle field on a face of the punch (b).

Summary

This work demonstrates the ability to form a 2-layer TFP preform on a doubly-curved part with a final orthotropic configuration. Only a minimal blank-holder setup was needed to form the preform without defects. The orthotropic orientation in the final configuration shows great improvement compared to forming of regular fibrous reinforcements. The design of the flat TFP pattern was obtained analytically by considering the inextensibility of the fibre tows. A first finite element model was proposed to simulate the forming of TFP preform without backing material. Based on a semi-discrete approach, the fibre tows are modelled explicitly using 2-node shear-flexible beam elements while the stitching yarn is modelled implicitly using an embedding constraint. It assumes the stitching yarn to act as a perfect bond between crossing fibre tows of adjacent layers. Additional linear torsional spring take into account the resistance to in-plane shear of the reinforcement.

In future work, the development of a numerical tool to determine the flat pattern of more complex parts is of interest. Besides, a model which takes into account the backing material is currently developed.

References

[1] X. Sun, J. P. -H. Belnoue, W.-T. Wang, B. C. Kim, S. R. Hallett, “Un-forming” fibre-steered preforms: Towards fast and reliable production of complex composites parts, Composi. Sci. Technol. 216 (2021) 109060. https://doi.org /10.1016/j.compscitech.2021.109060

[2] J. Simon, N. Hamila, C. Binetruy, S. Comas-Cardona, B. Masseteau, Design and numerical modelling strategy to form Tailored Fibre Placement preforms: Application to the tetrahedral part with orthotropic final configuration, Compos. Part A: Appl. Sci. Manuf. 158 (2022) 106952. https://doi.org /10.1016/j.compositesa.2022.106952

[3] A. Spickenheuer, M. Schulz, K. Gliesche, G. Heinrich, Using tailored fibre placement technology for stress adapted design of composite structures, Plastics, Rubber and Composites 37 (2008) 227-232. https://doi.org/10.1179/174328908X309448

[4] K. Uhlig, A. Spickenheuer, L. Bittrich, G. Heinrich, Development of a Highly Stressed Bladed Rotor Made of a CFRP Using the Tailored Fiber Placement Technology, Mech. Compos. Mater. 49 (2013) 201-210. https://doi.org/10.1007/s11029-013-9336-4
[5] K. Katagiri, S. Honda, S. Nakaya, T. Kimura, S. Yamaguchi, H. Sonomura, T. Ozaki, S. Kawakita, M. Takemura, K. Sasaki, Tensile strength of CFRP with curvilinearly arranged carbon fiber along the principal stress direction fabricated by the electrodeposition resin molding, Compos. Part A: Appl. Sci. Manuf. 143 (2021) 106271. https://doi.org/10.1016/j.compositesa.2021.106271
[6] P.J. Crothers, K. Drechsler, D. Feltin, I. Herszberg, T. Kruckenberg, Tailored fibre placement to minimise stress concentrations, Compos. Part A: Appl. Sci. Manuf. 28 (1997) 619-625. https://doi.org/10.1016/S1359-835X(97)00022-5
[7] K. Gliesche, Application of the tailored fibre placement (TFP) process for a local reinforcement on an “open-hole” tension plate from carbon/epoxy laminates, Compos. Sci. Technol. 63 (2003) 81-88. https://doi.org/10.1016/S0266-3538(02)00178-1
[8] E.G. Koricho, A. Khomenko, T. Fristedt, M. Haq, Innovative tailored fiber placement technique for enhanced damage resistance in notched composite laminate, Compos. Struct. 120 (2015) 378-385. https://doi.org/10.1016/j.compstruct.2014.10.016
[9] H. M. El-Dessouky, M. N. Saleh, M. Gautam, G. Han, R. J. Scaife, P. Potluri, Tailored fibre placement of commingled carbon-thermoplastic fibres for notch-insensitive composites, Compos. Struct. 214 (2019) 348-358. https://doi.org/10.1016/j.compstruct.2019.02.043
[10] K. Uhlig, A. Spickenheuer, K.Gliesche, I. Karb, Strength of CFRP open hole laminates made from NCF, TFP and braided preforms under cyclic tensile loading, Plastics, Rubber and Composites 39 (2010) 247-255. https://doi.org/10.1179/174328910X12647080902772
[11] M. Takezawa, Y. Otoguro, K. Matsuo, T. Shibutani, A. Sakurai, T. Maekawa, Fabrication of doubly-curved CFRP shell structures with control over fiber directions, Comput.-Aided Design. 136 (2021) 103028. https://doi.org/10.1016/j.cad.2021.103028
[12] G. Rihaczek, M. Klammer, O. Başnak, J. Petrš, B. Grisin, H. Dahy, S. Carosella, P. Middendorf, Curved Foldable Tailored Fiber Reinforcements for Moldless Customized Bio-Composite Structures. Proof of Concept: Biomimetic NFRP Stools, Polymers 12 (2020). https://doi.org/10.3390/polym12092000
[13] S. Allaoui, P. Boisse, S. Chatel, N. Hamila, G. Hivet, D. Soulat, E. Vidal-Salle, Experimental and numerical analyses of textile reinforcement forming of a tetrahedral shape, Compos. Part A: Appl. Sci. Manuf. 42) (2011) 612-622. https://doi.org/10.1016/j.compositesa.2011.02.001
[14] P. Ouagne, D. Soulat, J. Moothoo, E. Capelle, S. Gueret, Complex shape forming of a flax woven fabric; analysis of the tow buckling and misalignment defect, Composites Part A: Applied Science and Manufacturing. 51 (2013) 1-10. https://doi.org/10.1016/j.compositesa.2013.03.017
[15] M. Géradin, A. Cardona, Flexible Multibody Dynamics: A Finite Element Approach. Wiley-Blackwell, New York, 2001.
[16] M. Ritto-Corrêa, D. Camotim, On the differentiation of the Rodrigues formula and its significance for the vector-like parameterization of Reissner-Simo beam theory: Differentiation of Rodrigues formula, Int. J. Numer. Meth. Eng. 55) (2002) 1005-1032. https://doi.org/10.1002/nme.532
[17] A. Ibrahimbegović, F. Frey, I. Kožar, Computational aspects of vector-like parametrization of three-dimensional finite rotations, Int. J. Numer. Meth. Eng. 38 (1995) 3653-3673. https://doi.org/10.1002/nme.1620382107